SUBSURFACE MORPHOLOGY AND SCALING OF LUNAR IMPACT BASINS. K. Miljković[1], G. S. Collins[2], M. A. Wieczorek[3], B. C. Johnson[4], J. M. Soderblom[5], G. A. Neumann[6], and M. T. Zuber[5]. [1]Department of Applied Geology, Curtin University, Australia, [2]Department of Earth Sciences and Engineering, Imperial College London, UK, [3]Institut de Physique du Globe de Paris, France, [4]Department of Earth, Environmental and Planetary Sciences, Brown University, USA, [5]Department of Earth, Atmospheric and Planetary Sciences, Massachusetts Institute of Technology, USA, [6]Solar System Exploration Division, NASA/Goddard Space Flight Center, USA.

Introduction: Impact bombardment during the first billion years after the formation of the Moon produced at least several tens of craters larger than ~200 km in rim-to-rim diameter (impact basins). Given that some basins have multiple rings, and that portions of their defining morphological characteristics have been eroded, it was not always possible to provide a well-defined size for many of these basins.

Gravity measurements of the Moon obtained by the Gravity Recovery And Interior Laboratory (GRAIL) mission [1] provided the highest spatial resolution with global coverage to date, which allowed for a detailed analysis of the subsurface structure in lunar impact basins across the entire globe. In this study, we used maps of the lunar crustal thickness derived from the GRAIL gravity data [2] to define regions of crustal thinning (D_{thin}) observed in centers of lunar impact basins, which we demonstrated, represent an unambiguous measure of a basin size.

We numerically modeled basin-forming impacts using the iSALE-2D hydrocode, and compared the simulation results with the inferred subsurface morphology of lunar basins. Using the simulation results, we revised crater-size scaling laws applicable to lunar basins and quantified the sensitivity of the crust-mantle interface structure to plausible variations in target properties across the Moon (namely, temperature and crustal thickness).

Numerical impact methodology: We used the iSALE-2D hydrocode [3-5] to simulate the formation of lunar impact basins for a range of target properties typical for the Moon at the time of lunar basin formation. Impact simulations used nine different target temperature profiles, in combination with two assumed impact speeds (10 and 17 km/s) and three pre-impact crustal thicknesses (30, 45, and 60 km). All impact simulations used projectiles that were 15, 30, 45, 60 or 90-km in size, impacting the Moon at 10 or 17 km/s, which yield the entire size range of lunar impact basins except the South Pole-Aitken (SPA) basin. The methodology employed was similar to that in our previous work [7,8].

Fig. 1 shows an iSALE-2D simulation of a basin-forming impact made by a 45-km projectile moving at 17 km/s. Final basin morphology is represented by the diameters of crustal thinning and crustal thickening (D_{thin} and D_{thick}), the thickness of the crustal cap (h_{thin}), and crustal thickening at D_{thick} (h_{thick}).

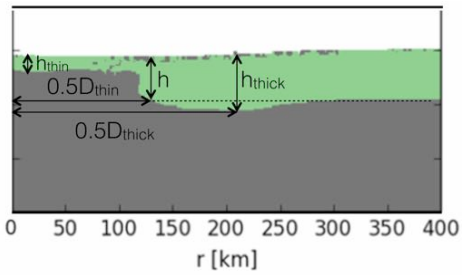

Fig. 1. Final basin morphology. h is the pre-impact crustal thickness (also up to where D_{thin} was measured).

Scaling of lunar impact basins: We used D_{thin} as a new baseline for a basin's size because it can be readily observed in gravity data, it is better preserved than surface topography, and it can be easily measured in impact simulations. We also used the impact coupling parameter C, instead of the transient crater diameter, as a baseline for the impact size, because C quantifies the impactor directly, and is less ambiquous. The coupling parameter C is defined as the product of the impactor diameter L and impactor velocity υ in the form of $L\upsilon^{\mu}$, assuming that the impactor and target densities are the same, and μ=0.58 [9]. Using our iSALE impact simulations, we derived power-law relationships between the coupling parameter C and the final basin morphology, represented via D_{thin} (C=A$D_{thin}^{\ b}$, Fig. 2).

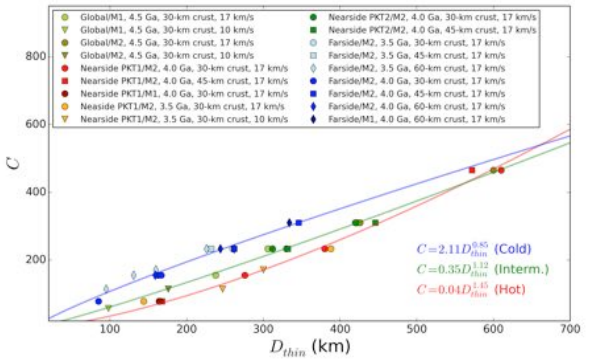

Fig. 2. Results from iSALE-2D simulations showing the C-D_{thin} relationship. "Global" denotes the temperature profile at 4.5 Ga ago, which represents a 1-D profile representative of both hemispheres of the Moon just after magma ocean crystallization. "Nearside" and "Farside" represent the two hemispheres at two later epochs (4.0 and 3.5 Ga) that differ as a result of the enhanced heat production on the nearside of the Moon

in the PKT. The enrichment in heat-producing elements in the nearside hemisphere was represented by two different profiles: PKT1 and PKT2; and designations M1 and M2 denote two different initial conditions that were tested for the mantle temperature profile (see [6-8] for details).

Fig. 2 shows that impacts into litospheres with similar temperature profiles followed a similar trend, and power-law fits were made for groups of impacts into a "hot" target (composed of impacts into targets with temperature profiles denoted as Nearside PKT1/M1, Nearside PKT1/M2, at 4.0 and 3.5 Ga), an "intermediate" temperature target (denoted as Global/M1, Global/M2 at 4.5 Ga, PKT2/M2 at 4.0 Ga), and a "cold" target (denoted as Farside/M1, Farside/M2 at 4.0 and 3.5 Ga), shown by the red, green and blue trend lines, respectively. Our results showed that the C-D_{thin} relationship depends predominantly on the target temperature, while the crustal thickness has a secondary effect.

We also grouped the GRAIL-observed lunar impact basins [10] into four groups based on their geographic location (and assumed target temperature). The nearside basins located within the PKT region were assumed to have formed in a hot target; the nearside basins outside of the PKT region, including the Orientale basin located on the limb, were assumed to have formed in an intermediate temperature target; and farside basins located both in the highlands region and within the SPA basin to have formed in a cold target.

Applying respective C-D_{thin} relationships to the GRAIL-observed lunar impact basins provides estimates of impact conditions that formed each of these basins. Assuming an average impact speed and impact angle, these relationships provide constraints on the projectile sizes that formed the observed lunar impact basins.

Subsurface morphology of impact basins: Numerical modeling results and GRAIL data showed there is no significant difference in D_{thin}/D_{thick} between impacts into different crustal thickness when using similar temperature profiles. However, simulations of basin-forming impacts into hot targets showed smaller D_{thin}/D_{thick} than basins that formed into cooler targets. This is likely a result of the target being weaker for a hotter crust, which allows for the inflow of more crustal materials into the basin during the collapse stage of the basin forming process. The range of simulated D_{thin}/D_{thick} ratios is comparable to those obtained for GRAIL-observed lunar impact basins (Fig. 3).

Consistent with observations, h_{thick}/h ratio is lower for the simulations of impact into a hot target than for those in a cold target. Similarly, our numerical modeling also suggested that the formation of lunar impact basins in a hot crust results in a larger h_{thin} than is the case for impacts in a cooler crust.

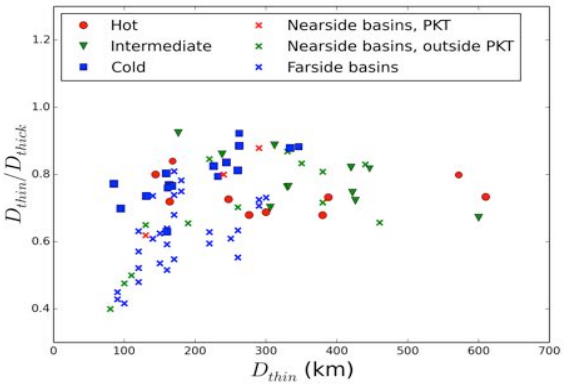

Fig. 3: The D_{thin}/D_{thick} ratio for iSALE simulations and GRAIL-observed lunar impact basins as a function of the crustal thinning diameter. Basins were separated according to their location, and compared against the numerical modeling results for hot, intermediate and cold targets (shown by filled symbols) comparable to the Moon at the time the majority of lunar basins formed.

Conclusions: Understanding of the effects that target properties have on the impact-basin formation process leads to a refinement of impact scaling laws, which are a very useful tool for the conversion from an observed basin size to its impactor properties. Our C-D_{thin} relationships provide new scaling between directly observed impact basins by GRAIL and probable impact conditions that formed these basins.

Our analysis of lunar basin subsurface morphology suggests that the target temperature affects both the final basin size and the extent of the crustal thinning, mantle uplift, thickening of the crust surrounding the mantle uplift, and thickness of the crustal cap that covers up the mantle uplift.

References: [1] Zuber M.T. et al. (2013) *Science* 339, 668–671. [2] Wieczorek M.A. et al. (2013) *Science* 339, 671-675. [3] Amsden A.A. et al. (1980) *LANL Report* LA-8095, 105. [4] Collins G.S. et al. (2004) *Meteorit. Planet. Sci.* 39, 217–231. [5] Wünnemann K. et al. (2006) *Icarus* 180, 514–251. [6] Laneuville, M. et al. (2013) *J. Gephys. Res.* 118, 1435-1452. [7] Miljković, K., et al. (2013) *Science* 342, 724–726. [8] Miljković, K. et al. (2015) *Earth Planet. Sci. Lett.* 409, 243–251. [9] Holsapple K.A. and Schmidt R.M. (1987) *J. Geophys. Res.* 92(B7) 6350–6376. [10] Neumann G.A. et al. (2015) Sci. Adv. 1, 9, e1500852.

Acknowledgements: We gratefully acknowledge the developers of iSALE-2D (www.isale-code.de/projects/ iSALE). The GRAIL mission is supported by the NASA Discovery Program and is performed under contract to MIT and JPL, Caltech.